Between Lives and Economy: Optimal COVID-19 Containment Policy in Open Economies*

Wen-Tai Hsu† Hsuan-Chih (Luke) Lin‡ Han Yang§

February 21, 2021

Abstract

This paper studies optimal containment policy for combating a pandemic in an open-economy context. It does so via quantitative analyses using a model that incorporates a standard epidemiological compartmental model in a multi-country, multi-sector Ricardian model of international trade with input-output linkages. We devise a novel approach in computing optimal national policies in the long run and contrast these policies with a baseline in which countries maintain their current policies until sufficient vaccine rollout. We find that (1) a laissez-faire policy might not be all that bad in terms of long-run real income, but it is a drastically worse policy in welfare terms because of risk aversion; (2) the welfare gains under optimal policies are asymmetric as the gains for the set of countries that should tighten up the containment measures are much larger than the gains for those that should relax; (3) international trade acts as a buffer to welfare losses from the pandemic if a country's average work-from-home capacity is high, and it also implies substantially different optimal policies in welfare terms from closed-economy settings.

Keywords: COVID-19, pandemic, welfare analysis, disease dynamics, effective reproduction number, containment policy, optimal policy, open economy, trade

JEL Classification: I18; F11; F40; E27

*We thank Ippei Fujiwara, Matt Shapiro, Michael Zheng Song, and seminar participants in Academia Sinica, Singapore Management University, and the Virtual East Asia Macroeconomic Seminar Series. The online appendix to this paper is available at http://wthsu.com.

†School of Economics, Singapore Management University. Email: wentaihsu@smu.edu.sg.

‡Institute of Economics, Academia Sinica, Taiwan. Email: linhc@econ.sinica.edu.tw.

§Institute of Economics, Academia Sinica, Taiwan. Email: hanyang@econ.sinica.edu.tw.

1 Introduction

One of the most important questions in a pandemic such as COVID-19, the one we face now, is how stringent the containment policies should be. There are heated debates on this in many countries, and a large cross-country variation in the stringency of containment policies is apparent. The key tradeoff is obvious: lives vs. economy. But striking the right balance is not a simple task due to the complexity of the economy and its complicated interaction with the disease's epidemiological evolution. There has been a surge of research on optimal containment policy in macroeconomics literature, but these studies are mostly, if not all, in closed-economy contexts. As the global economy is interlinked across countries, a country's containment policy may have repercussions on other countries' economies through various trade linkages, which may, in turn, affect the considerations of other countries' containment policies and the ensuing health outcomes.

This paper attempts to answer questions regarding optimal containment policy in an open-economy context. We do so by conducting quantitative analyses using a model that incorporates a standard epidemiological compartmental model (**S**usceptible-**I**nfected-**R**ecovered-**D**eceased; SIRD) in a multi-country, multi-sector Ricardian model of international trade with full-fledged input-output linkages (Eaton and Kortum (2002) and Caliendo and Parro (2015)). In particular, our model builds on that of Caliendo and Parro (2015) by adding how the pandemic shocks different sectors and countries differently due to the heterogeneity in containment policy and work-from-home (henceforth WFH) capacity, which in turn reshapes comparative advantages and the distribution of sectoral employment. The rate of disease transmission is then influenced by such changes in sectoral employment through workplace interactions, and the SIRD law of motion then influences the next-period labor supply. Thus, this model features two-way dynamic influences between the economy and the pandemic. It also features cross-country externality of containment policies through trade linkages.

Our model is calibrated to the pre-COVID-19 economy, mainly using the World Input-Output Database (WIOD), in which there are 42 countries. Our key disease transmission parameters are disciplined by the data on the total confirmed cases. When computing optimal policies in such a multi-country, multi-sector, multi-period framework, the key challenge is to devise a reasonable and tractable approach to reduce the huge space of candidate policies to facilitate efficient computation of optimal policies. To this end, we use the effective reproduction number R_e as the policy target for each country instead of optimizing over the entire time paths of policies for the 42 countries, which is infeasible. This is a reasonable target/representation, as R_e reflects the speed of disease spread and is the central concern for epidemiologists and doctors who lead government responses. Moreover, targeting R_e implies that the containment measures should be stringent initially and generally become more lenient over time, which is a pattern found in several recent studies in the macroeconomic literature which focus on the dynamics of optimal policies in closed-economy contexts; see, e.g., Alvarez et al. (2020) and Jones et al. (2020).

Our welfare measure is equivalent to the sum of individual expected utilities, which are concerned with risks in a pandemic, as, ex ante, no one knows how he/she would fare during the pandemic. In the special case where people are risk-neutral, our welfare measure is reduced to real income, and the cost of death is simply the long-run loss in real income due to the loss of labor endowment. Under general risk aversion, people dislike extreme outcomes; hence an increase in the probabilities of death or infection worsens welfare beyond the loss in real income.

As a pandemic involves a tradeoff between lives and economy, the considerations for an optimal policy are necessarily long-run. To consider the long-run effects of containment policies and compare these with optimal policies, we compute a baseline in which countries maintain their current policies until the pandemic ends with sufficient vaccination being rolled out. We compute optimal policies in two steps. In the first step, we consider a global planner who seeks to maximize global welfare by deciding on an R_e that applies to all countries. In this step, we find that most countries' welfare and real income improves under an optimal uniform R_e, and in terms of global welfare and real income, there is an interesting divergence when the policy is laissez-faire. In this case, there are actually gains in real income compared with the baseline, even though this is still sub-optimal, as the optimal one requires a relatively stringent policy. However, the welfare loss compared with the baseline under the laissez-faire policy is substantial. As deaths are extreme outcomes disliked by risk-averse agents, the cost of mortality is amplified in welfare terms beyond the associated real-income losses. Our quantitative results suggest that such amplification under laissez-faire policy is so large that it overcomes the real-income gains (for those who remain alive) under this policy to entail a welfare loss.

In the second step, we solve each country's optimal effective reproduction number $R_{e,i}$ given other countries' optimal choices $R_{e,-i}$; this is, indeed, a Nash equilibrium of national optimal policies. Information from the first step helps ease the computational burden in this step as it suggests how the grid search can be efficiently conducted. We find that a majority of countries need to tighten up, whereas five countries need to relax. There is an interesting asymmetry in which welfare gains are much larger for those that need to tighten up than for those that need to relax. The key reasoning behind this asymmetry is again that the long-run cost of mortality factors in both the real income and welfare, but it weighs more in welfare. We defer detailed explanations to Section 4.3.

Finally, we find that international trade acts as a buffer to welfare losses from the pandemic if a country's average WFH capacity is high and that the optimal policies under closed economies differ substantially from those under open economies in welfare terms. The average difference in welfare improvement under optimal policies between closed and open economies is 72% relative to the welfare improvement in open economies.

Related Literature. There has been a surge of research studying optimal containment policies: these studies embed variants of the classic SIR model proposed by Kermack et al. (1927) into macroeconomic models to study various aspects of the tradeoff between lives and economy. See, for examples, Acemoglu et al. (2020), Alvarez et al. (2020), Atkeson (2020), Atkeson et al. (2020), Eichenbaum et al. (2020), Farboodi et al. (2020), Jones et al. (2020), Krueger et al. (2020), and Piguillem and Shi (2020). Our work differs from all of the above in our focus on analyzing optimal containment policies in an open-economy context. A particularly closely related work is that by Budish (2020) who formulates a static optimization problem using $R_e < 1$ as a constraint. Our work differs as R_e is used as a policy target (rather than a constraint) in a dynamic setting. Interestingly, the optimal effective reproduction numbers that we find are all less than 1 in all scenarios.

Also closely related are the studies by Antrás et al. (2020), Fajgelbaum et al. (2020), and Argente et al. (2020) who all consider disease dynamics in a general equilibrium model of trade in either a city or an international-trade setting. Our work differs from Antrás et al. (2020) mainly due to our focus on optimal containment policies, and differs from Fajgelbaum et al. (2020) and Argente et al. (2020) due to our focus on country-level containment policies. Broadly related work includes Chen et al. (2020), Bonadio et al. (2020), and Eppinger et al. (2020), who study the role of trade and/or input-output linkages in the pandemic's shocks on the economy. However, these studies do not incorporate disease dynamics or analyze optimal containment policies, which are our main focuses.

The rest of the paper is organized as follows. Section 2 describes the model, Section 3 introduces the data and how the model is calibrated, Section 4 presents the quantitative analyses on containment policies, and Section 5 concludes.

2 Model

Our model incorporates the evolution of the pandemic and the labor productivity shocks arising from the pandemic into a Caliendo and Parro (2015) trade model, a general equilibrium Eaton and Kortum (2002) model with multiple sectors and full-fledged input-output linkages.

2.1 Preference

There are K countries, each of which has a population of $N_i, i \in \{1, 2, ..., K\}$. There are J sectors, each of which consists of a unit continuum of varieties. The final-good consumption of an individual in country i in period t, $q_{i,t}$, consists of a Cobb-Douglas bundle of sectoral goods $q_{i,t}^{F,j}$:

$$q_{i,t} = \prod_{j=1}^{J} (q_{i,t}^{F,j})^{\alpha_i^j},$$

and each sectoral good is made of a CES composite:

$$q_{i,t}^{F,j} = \left[\int_0^1 q_{i,t}^{F,j}(\omega)^{\frac{\kappa-1}{\kappa}} d\omega \right]^{\frac{\kappa}{1-\kappa}}, \tag{1}$$

where $q_{i,t}^{F,j}(\omega)$ is the amount of variety ω used for final consumption, and $\kappa > 1$ is the elasticity of substitution. The life-time utility of an individual (in a dynastic sense) is given by

$$u_i = \sum_{t=0}^{\infty} \rho^t u\left(q_{i,t}\right),$$

where ρ is the discount factor, and u is a concave and strictly increasing function.

2.2 Production

Labor is the fundamental input for production, and the production in each sector potentially uses intermediate inputs from all sectors. Countries differ in their productivities across sectors and varieties. Production technology exhibits constant returns to scale. Both the goods and factor markets are perfectly competitive. Let $M_{i,t}^j(\omega)$ denote the use of the composite intermediate goods by the firms producing variety ω in sector j and country i; it is made of a Cobb-Douglas composite:

$$M_{i,t}^j = \prod_{l=1}^{j} (q_{i,t}^{M,l})^{\gamma_i^{j,l}}, \tag{2}$$

where the sectoral good $q_{i,t}^{M,l}$ is made by the same CES aggregator across varieties as in (1) with the inputs being $q_{i,t}^{M,j}(.)$. Note that each sector j's intermediate composite's expenditure share on sector l's good, $\gamma_i^{j,l}$, is country-specific.

Denote a country-sector-time-specific pandemic shock parameter on the production function by $B_{i,t}^j$, which will be specified later; for the pre-COVID-19 economy, this term drops out as $B_{i,t}^j = 1$. The production function of a variety ω in sector j and country i is given by

$$y_{i,t}^j(\omega) = \frac{z_i^j(\omega) \left[B_{i,t}^j L_{i,t}^j(\omega) \right]^{\beta_i^j} M_{i,t}^j(\omega)^{1-\beta_i^j}}{(\beta_i^j)^{\beta_i^j} (1-\beta_i^j)^{1-\beta_i^j}}, \tag{3}$$

where $L^j_{i,t}(\omega)$ is the labor hired for this variety, β^j_i is the labor share, and the Hicks-neutral productivity $z^j_i(\omega)$ is drawn *i.i.d.* from a Fréchet distribution: $\Pr(x < z) = \exp(-T^j_i z^{-\theta})$, where $T^j_i > 0$ is the country-sector-specific scaling parameter and $\theta > 1$ is the shape parameter. The draws are also independent across countries and sectors. The denominator of production function (3) is simply a normalizing constant for a clean expression of the unit cost.

The trade cost is of the standard iceberg-cost form: to deliver one unit of sector-j variety from country i to country n, $\tau^j_{i,n} \geq 1$ units are required to ship. We assume that trade is balanced. The unit cost of delivering a good from country i to country n is $c^j_{i,t}\tau^j_{i,n}/z^j_{i,t}(\omega)$, where

$$c^j_{i,t} = \left(\frac{w_{i,t}}{B^j_{i,t}}\right)^{\beta^j_i} (P^{M,j}_{i,t})^{1-\beta^j_i},$$

where $w_{i,t}$ and $P^{M,j}_{i,t}$ are country i's wages and its sector j's price for obtaining the intermediate input bundle specified in (2), respectively. Here, $c^j_{i,t}$ is indeed the unit cost to produce a sector j variety under unit productivity. In this environment with perfect competition and constant returns to scale, prices equal the (delivered) marginal costs, and each country n buys from the cheapest source: $p^j_{n,t}(\omega) = \min_i \left\{c^j_{i,t}\tau^j_{i,n}/z^j_{i,t}(\omega)\right\}$. Standard derivation yields the price indices:

$$P^j_{i,t} = \left(\int_0^1 p^j_{i,t}(\omega)^{1-\kappa}\right)^{\frac{1}{1-\kappa}}, \quad P^{M,j}_{i,t} = \prod_{l=1}^{J}\left[P^l_{i,t}\right]^{\gamma^{j,l}_i}, \quad P_{i,t} = \prod_{j=1}^{J}\left[P^j_{i,t}\right]^{\alpha^j_i}. \tag{4}$$

2.3 Pandemic and Economy

We incorporate a standard epidemiological model, i.e., an SIRD model, as follows. At any period t, the population of country i, N_i, consists of people who are **S**usceptible ($S_{i,t}$, have not been exposed to the disease), **I**nfectious ($I_{i,t}$, have contracted the disease), **R**ecovered ($R_{i,t}$, have recovered and are immune), and **D**eceased ($D_{i,t}$, died from the disease). That is, $N_i = S_{i,t} + I_{i,t} + R_{i,t} + D_{i,t}$. The epidemiology is characterized by

$$\begin{aligned}
S_{i,t+1} &= S_{i,t} - T_{i,t} \\
I_{i,t+1} &= I_{i,t} + T_{i,t} - (\pi^r + \pi^d_{i,t})I_{i,t} \\
R_{i,t+1} &= R_{i,t} + \pi^r I_{i,t} \\
D_{i,t+1} &= D_{i,t} + \pi^d_{i,t} I_{i,t},
\end{aligned}$$

where π^r and $\pi^d_{i,t}$ are the probabilities of recovering from the infectious status in a period t and of death, respectively, and $T_{i,t}$ is the number of newly infected people. To capture the fact that the strain of the number of infectious people on the medical system generally increases the mortality rate $\pi^d_{i,t}$, we assume $\pi^d_{i,t} = \pi^d + \delta I_{i,t}/N_i$, where $\delta > 0$ and π^d is the base mortality rate. This linear form is also assumed by Alvarez et al. (2020).

Next we link the SIRD model back to our economic environment. As deaths reduce the labor force, and infections negatively affect individuals' labor supply, the effective labor force at time t is

$$L_{i,t} = S_{i,t} + R_{i,t} + \alpha^I I_{i,t}, \tag{5}$$

where $1 - \alpha^I$ fraction of labor time is lost from contracting the disease.

Let $\mu_i^j \in [0, 1]$ be the capacity to work from home for sector j in country i, and let $\eta_{i,t} \in [0, 1]$ be the degree of the containment measure in country i at time t; $\eta_{i,t} = 1$ means a total lockdown whereas $\eta_{i,t} = 0$ means totally laissez-faire, but a containment policy can be anywhere in between. Assume that during a pandemic, workers who can work from home (the fraction of such workers is μ_i^j) work from home regardless of the containment policy, but for those workers who are unable to work from home, they must still meet in workplaces if allowed. If a country's containment measure is $\eta_{i,t}$, then $\eta_{i,t}(1 - \mu_i^j)$ fraction of workers are locked away. Only those who are not locked away still meet; the fraction of such workers is $(1 - \eta_{i,t})(1 - \mu_i^j)$. Assume that the containment measure also applies to interactions in general activities. The number of newly infected individuals is given by

$$T_{i,t} = \frac{(1 - \eta_{i,t})\pi_i^I S_{i,t} I_{i,t} + \pi_i^L \times \sum_{j=1}^{J} \left[(1 - \eta_{i,t})(1 - \mu_i^j)\ell_{i,t}^j \right] S_{i,t} I_{i,t}}{N_i}, \tag{6}$$

where $\ell_{i,t}^j$ is sector j's employment share in country i at time t, and π_i^L and π_i^I are the infection rates from interactions at workplaces and from general activities other than working, respectively. Similar forms have been used in Eichenbaum et al. (2020) and Jones et al. (2020). The key difference from these macroeconomic models is that instead of focusing on how households react to the pandemic by cutting their consumption and labor supply, we expand in the country and sector dimensions to study how sectoral employment shares $\ell_{i,t}^j$ react to changing circumstances of containment policies, augmented by the sectoral WFH capacity, and subsequently affect the speed of disease spread.

As the effective labor time supplied per worker in sector j and country i is reduced to $\mu_i^j + (1 - \eta_{i,t})(1 - \mu_i^j) = 1 - \eta_{i,t}(1 - \mu_i^j)$, the employers can pay the full wages even when workers' effective time supplied is reduced; or, the employers can choose to lay off workers or hire part-time. In the former case, employers absorb the shocks directly, whereas the workers absorb the shocks in the latter case. Both scenarios are present in reality, and their effects are similar. To keep the model tractable, we focus on the former case. Thus, the pandemic-shock parameter in the production function (3) is $B_{i,t}^j \equiv 1 - \eta_{i,t}(1 - \mu_i^j) \in [0, 1]$. In the case where $\eta_{i,t} = 0$ (as would be the case when there is no pandemic or when a laissez-faire policy is adopted), $B_{i,t}^j = 1$.

Observing (3) and (6), a more stringent containment measure (higher $\eta_{i,t}$) reduces infections but hurts production; both effects are mitigated if the sector of concern has a larger WFH capacity. Both effects also differ across countries due to the differences in infection probabilities $\{\pi_i^I, \pi_i^L\}$ and country-specific production parameters. The international division of labor reflected by $\{\ell_{i,t}^j\}$ provides an *endogenous source* of cross-country heterogeneity in the rate of transmission. We allow for π_i^I and π_i^L to differ across countries because these may reflect country-specific environments such as geography, climate, or culture that potentially affect the rate of disease transmission given the same intensity of interactions in workplaces and in general.

Assuming $\kappa < \theta + 1$, the price index of a sectoral good is given by

$$P_{n,t}^j = \zeta \left(\sum_{k=1}^{K} T_k^j \left[\left(w_{k,t}/B_{k,t}^j \right)^{\beta_k^j} \left(P_{k,t}^{M,j} \right)^{1-\beta_k^j} \tau_{k,n}^j \right]^{-\theta} \right)^{-\frac{1}{\theta}}, \tag{7}$$

where $\zeta \equiv \left[\Gamma \left(\frac{\theta+1-\kappa}{\theta} \right) \right]^{1/(1-\kappa)}$, and the expenditure share of sector-j goods that country n purchases from country i is given by

$$\pi_{i,n,t}^j = \frac{T_i^j \left[\left(w_{i,t}/B_{i,t}^j \right)^{\beta_i^j} \left(P_{i,t}^{M,j} \right)^{1-\beta_i^j} \tau_{i,n}^j \right]^{-\theta}}{\sum_{k=1}^{K} T_k^j \left[\left(w_{k,t}/B_{k,t}^j \right)^{\beta_k^j} \left(P_{k,t}^{M,j} \right)^{1-\beta_k^j} \tau_{k,n}^j \right]^{-\theta}}. \tag{8}$$

Containment policies combined with WFH capacity reshape comparative advantages. If all countries adopt the same containment policy, a country i gains a comparative advantage in those high μ_i^j sectors as $B_{i,t}^j$'s are larger. This means that a country's containment policy affects its *own and other* countries' distributions of sectoral employment, which subsequently change their rates of disease spread, which in turn affect the labor supply (and hence wages and comparative advantages) in the next period. Such a cross-country externality of containment policies cannot be captured in a closed-economy model. Moreover, this model is not a Caliendo-Parro model repeatedly shocked by a disease evolution that runs independently. Instead, it features a dynamic mechanism in which the economic situations also change the speed of disease spread.

2.4 Equilibrium

Let $R_{i,t}^j$ denote the total revenue of country i's sector j, $X_{n,t}^j$ denote the total expenditure of country n on goods in sector j, and $X_{n,t}$ denote the total expenditure of country n. By definition, $R_{i,t}^j = \sum_{n=1}^{K} \pi_{i,n,t}^j X_{n,t}^j$. The market clearing condition for labor is therefore

$$w_{i,t} L_{i,t} = \sum_{j=1}^{J} \beta_i^j R_{i,t}^j = \sum_{j=1}^{J} \sum_{n=1}^{K} \beta_i^j \pi_{i,n,t}^j X_{n,t}^j. \tag{9}$$

By the definition of $X^j_{i,t}$,

$$X^j_{i,t} = \underbrace{\underbrace{\alpha^j_i w_{i,t} L_{i,t}}_{\text{consumption}} + \sum_{l=1}^{J} \underbrace{\gamma^{l,j}_i (1-\beta^l_i) R^l_{i,t}}_{\text{as intermediate for sector } l}}_{\text{total demand}}$$

$$= \underbrace{\underbrace{\alpha^j_i w_{i,t} L_{i,t}}_{\text{consumption}} + \sum_{l=1}^{J} \underbrace{\gamma^{l,j}_i (1-\beta^l_i) \sum_{n=1}^{K} \pi^l_{i,n,t} X^l_{n,t}}_{\text{as intermediate for sector } l}}_{\text{total demand}} . \tag{10}$$

This is indeed a system of linear equations with consumption as intercepts.

A brief description of the equilibrium algorithm is given as follows; the detailed algorithm is relegated to the online appendix.[1] We first solve the equilibrium at time t given the SIRD objects $\{S_{i,t}, I_{i,t}, R_{i,t}, D_{i,t}\}$ and $\{L_{i,t}\}$ from (5). Given wages $\{w_{i,t}\}$, $\{P^{M,j}_{i,t}, P_{i,t}, P^j_{i,t}, \pi^j_{i,n,t}, X^j_{k,t}\}$ are obtained from (4), (7), (8), and (10). Equilibrium wages are obtained from (9). In particular, sectoral employment shares are computed by $\ell^j_{i,t} = \beta^j_i R^j_{i,t} / \sum_{l=1}^{J} \beta^l_i R^l_{i,t}$. Then, the next-period SIRD objects are obtained from the law of motion specified in Section 2.3 with the number of newly infected $\{T_{i,t}\}$ given by (6).

2.5 Welfare

A pandemic poses uncertainty to individuals as to how one would fare in terms of the compartments $\{S_{i,t}, I_{i,t}, R_{i,t}, D_{i,t}\}$. For a country i, its welfare is measured by the sum of individual expected life-time utility in which everyone's probability of falling into each compartment is given by the fraction of people in that compartment.[2] As consumption is given by real income $w_{i,t}/P_{i,t}$, the welfare of country i is given by

$$U_i = \sum_{t=0}^{\infty} \rho^t \left[(S_{i,t} + R_{i,t})\, u\left(\frac{w_{i,t}}{P_{i,t}}\right) + I_{i,t} u\left(\frac{\alpha^I w_{i,t}}{P_{i,t}}\right) + D_{i,t} u\,(0) \right].$$

Note that the concavity of u reflects the degree of risk aversion. This formulation treats an individual's death as a complete loss of labor, which implies zero income and hence zero consumption. If $u(0) = 0$, then the loss from death is simply the loss of utility from the other two outcomes before one's death. When $u(0) \neq 0$, its value actually reflects the psychological cost that one may have toward death. As it is difficult to calibrate psychological costs, we set $u(0) = 0$ for a relatively clear benchmark. In most cases, it is easy to predict the directions of how our results would change when psychological costs are incorporated.

[1] The online appendix is available at https://wthsu.com.

[2] Note that this probability is unconditional viewed at time 0.

When u is linear, i.e., the risk-neutral case, a country i's welfare actually becomes the present value of aggregate real income: $U_i = \sum_{t=0}^{\infty} \rho^t \frac{w_{i,t} L_{i,t}}{P_{i,t}}$. The global welfare is defined analogously:

$$U = \sum_{i=1}^{K} U_i = \sum_{i=1}^{K} \sum_{t=0}^{\infty} \rho^t \left[(S_{i,t} + R_{i,t})\, u\left(\frac{w_{i,t}}{P_{i,t}}\right) + I_{i,t} u\left(\frac{\alpha^I w_{i,t}}{P_{i,t}}\right) + D_{i,t} u\left(0\right) \right]. \tag{11}$$

As U_i is already the aggregate welfare that takes into account the population in country i, the global welfare is simply the sum of individual countries' welfare.

3 Quantification

This section briefly describes how we quantify the model. The full details of the quantification are relegated to the appendix. For our quantitative analyses, we set the per-period utility as

$$u(q) = \frac{(q+1)^{1-\sigma} - 1}{1-\sigma}.$$

We choose this functional form for three reasons. First, this specification is similar to the CRRA (constant relative risk aversion) utility if the term $q+1$ is replaced with q. Thus, it is approximately CRRA when q is large; the parameter σ measures the degree of relative risk aversion. Second, $u(0) = 0$, which satisfies our requirement to leave psychological costs out of the model; note that the exact CRRA utility entails $\lim_{q \to 0} u(q) \to -\infty$ when $\sigma \geq 1$ and is therefore not implementable. Third, $\sigma = 0$ corresponds to the risk-neutral case. Following Low and Pistaferri (2015), the relative risk aversion σ is set to 1.5. Following Farboodi et al. (2020), we set the annual discount rate as 0.95; as daily data is used, $\rho = 0.95^{\frac{1}{365}} \approx 0.99986$.

The economic environment is calibrated to the world economy prior to the COVID-19 pandemic using the World Input-Output Database (WIOD) and Centre d'Études Prospectives et d'Informations Internationales (CEPII) data. There are 42 countries in this data set. We aggregate the 56 WIOD industries into six sectors (one primary sector, three manufacturing sectors, and two service sectors distinguished by high skill and low skill). Hence, $K = 42$ and $J = 6$.

The share parameters $\{\alpha_i^j, \beta_i^j, \gamma_i^{j,l}\}$ in the utility and production functions are calibrated using the input-output table information in the WIOD. Given the data on trade shares and geography from the WIOD and CEPII, the model's gravity equations and hence trade costs $\{\tau_{i,n}^j\}$ can be estimated. Following Simonovska and Waugh (2014), we set the value of trade elasticity $\theta = 4$. Given trade elasticity, estimated trade costs, the share parameters $\{\alpha_i^j, \beta_i^j, \gamma_i^{j,l}\}$, and data on wages obtained from the Social Economic Account in WIOD, the productivity parameters $\{T_i^j\}$ can then be backed out using the model structure.

The values of WFH capacity $\{\mu_i^j\}$ are obtained from Dingel and Neiman (2020), who compute such capacity by occupation and then aggregate to NAICS industries. We map their 3-digit

NAICS results to WIOD industries and our aggregate sectors. The containment measures $\{\eta_{i,t}\}$ are obtained from the *Stringency Index* by the Oxford COVID-19 Government Response Tracker (OxCGRT; Hale et al. 2020) at a daily frequency. This index summarizes a government's responses in terms of various closures and containment, including school or workplace closures, stay-at-home requirements, border control, and restrictions on gathering, public events, public transport, and internal movements, as well as public information campaigns.

Next, we turn to the epidemiological parameters $\{\pi^r, \pi^d, \delta, \pi_i^I, \pi_i^L, \alpha^I, I_{i,0}\}$. As in Atkeson (2020) and several other macro-SIRD models, we set $\pi^r + \pi^d = 1/18$, which means that it takes on average 18 days to either recover or die from the infection. From Liang et al. (2020), the base mortality rate is set at $\pi^d = 0.037 \times \frac{1}{18}$.[3] Following Alvarez et al. (2020), we set $\delta = 0.05 \times \frac{1}{18}$. As a WHO (2020) COVID-19 Situation Report indicates that asymptotic and mild cases account for about 80% of the infections, we set $\alpha^I = 0.8$.

For our purpose, it is important to account for the variations in the rate of disease reproduction across countries, the key parameters for which are the two infection probabilities $\{\pi_i^I, \pi_i^L\}$ in (6). Also, for the epidemiological evolution to commence, an estimate of $I_{i,0}$ is required (as $S_{i,0} = N_i - I_{i,0}$ and $R_{i,0} = D_{i,0} = 0$); $I_{i,0}$ is generally unknown and must be estimated because the society might be unaware of, unprepared for, or on low alert for the disease so that the number of the first few reported cases may be quite off. For each country, parameters $\{\pi_i^I, \pi_i^L, I_{i,0}\}$ are estimated by the non-linear least-squares method that minimizes the squared distance in the total confirmed cases between data and model. The data on total confirmed cases are downloaded from the Humanitarian Data Exchange website.[4] Our estimated model fits the data reasonably well, as the cross-country average and standard deviation of R^2 are 0.88 and 0.067, respectively.

4 Quantitative Analyses on Containment Policies

For equilibrium computation and simulations for counter-factuals, we simulate the evolution of the economy and disease from a pre-COVID-19 world with pandemic shocks $\{B_{i,t}^j\}$. The first date ($t = 0$) is set as January 1, 2020, which is the first date for which the Stringency Index is available. Assume that the disease evolution for a country i starts at the date on which the total confirmed cases in the data exceed 50; this date is denoted as t_i^*. Then, the estimated $I_{i,0}$ is applied to the previous day ($t_i^* - 1$); for all days between January 1, 2020 and that previous day, $I_{i,t} = R_{i,t} = D_{i,t} = 0$ and $S_{i,t} = N_{i,t}$. When this paper was written, the latest date for which the Stringency Index was available for all countries in our data set was November 16, 2020.

[3] This number is estimated as a case mortality rate. This choice of mortality rate is consistent with our estimation of some key parameters using official data on the number of cases as described below.

[4] See Dong et al. (2020) (`https://data.humdata.org/dataset/novel-coronavirus-2019-ncov-cases`) for data.

The online appendix shows a short-run counter-factual analysis in which all countries imitate South Korea's containment policies up to November 16. The Korean policies turn out to be too stringent for a majority of countries as the economic values of saved lives are not sufficient to cover the losses of real income in this 11-month span. The problem with that analysis is obvious: the losses of real income are temporary, but the loss of lives must be evaluated in the long run. As our focus is on optimal containment policies, our analysis is necessarily long-run.

4.1 Effective Reproduction Numbers and the Long-run Environment

A key object in epidemiology is the effective reproduction number $R_{e,i,t}$, which is the number of cases directly generated from one case, is given by

$$R_{e,i,t} \equiv \frac{T_{i,t}}{I_{i,t}} \times 18 = (1-\eta_{i,t}) \left[\pi_i^I + \pi_i^L \times \sum_{j=1}^{J} (1-\mu_i^j) \ell_{i,t}^j \right] \times 18 \times \frac{S_{i,t}}{N_i}. \tag{12}$$

To see the significance of $R_{e,i,t}$, note that the term in the bracket is actually the rate of transmission (the rate of getting infected from Susceptible); when this rate is divided by the rate of leaving the infectious compartment, $1/18$, it entails the number of cases directly generated from one case at the onset of the disease and without government intervention (so $S_{i,t}/N_i = 1$ and $1-\eta_{i,t} = 1$). This is actually the famous basic reproduction number R_0, although in our model it is actually country-specific and time-varying (denoted as $R_{0,i,t}$) due to cross-country differences in $\{\pi_i^I, \pi_i^L \, \ell_{i,t}^j\}$ and the time variability in $\ell_{i,t}^j$. Then, the effective number of cases generated directly from one case is the product of $R_{0,i,t}$ and the fraction of "effective" susceptible people given by $(1-\eta_{i,t})S_{i,t}/N_{i,t}$.

From (12), it is easy to understand two main strategies for combating the disease. One approach is to impose sufficiently stringent containment measures so that the effective reproduction number goes below 1, in which case the disease spread slows down, and to wait for vaccines. The second approach is to use various ways to "protect the vulnerable" while letting the disease spread faster in the hope for herd immunity. In the first approach, $1-\eta_{i,t}$ remains low, but the fraction of susceptible in the population remains high; this approach would not be feasible without reasonable prospects for vaccines in the near future. In the second approach, $1-\eta_{i,t}$ is high, but $S_{i,t}/N_i$ goes down faster and when $S_{i,t}/N_i$ is so low that $R_{e,i,t} < 1$ even when there is no containment measure ($\eta_{i,t} = 0$), herd immunity is reached.

Figure 1 shows the over-time average of both $R_{0,i,t}$ and $R_{e,i,t}$ for each country between the onset of the disease spread t_i^* and November 16, 2020. There is considerable cross-country variation in the basic reproduction number with most countries ranging from 1 to 4. However, when it comes to the effective reproduction number, the variation is much smaller. Most importantly,

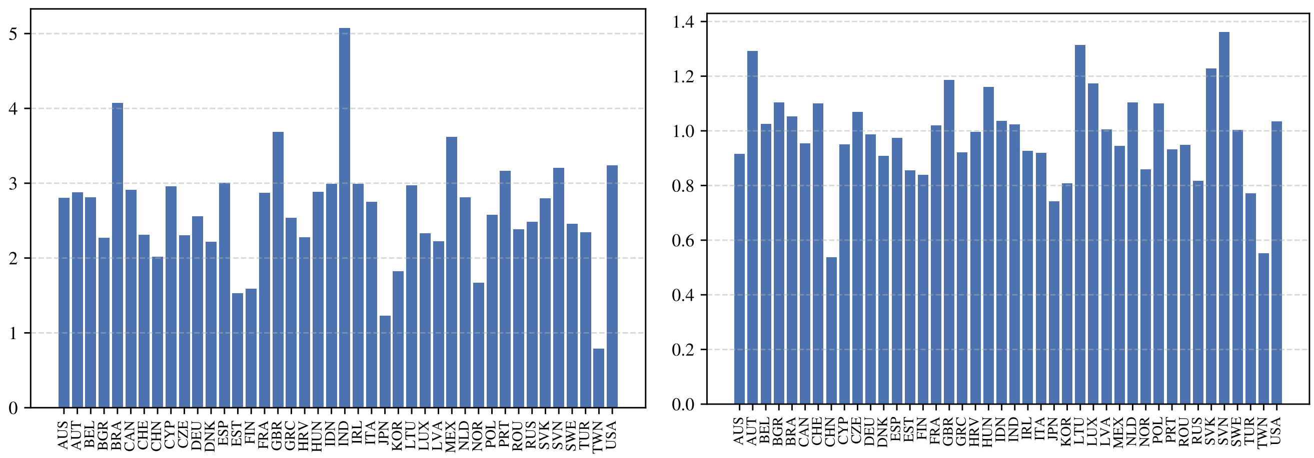

(a) Average basic reproduction number

(b) Average effective reproduction number

Figure 1: Current $\bar{R}_{e,i}$ and Results under a Uniform $\widetilde{R}_e$

the scale of average $R_{e,i,t}$ is much smaller than that of average $R_{0,i,t}$ with the former hovering around 1. This indicates strong containment effort from governments across the globe in slowing disease spread. It is then clear that most governments have adopted strategies with the prospect for vaccines in mind.

Even though several vaccines have been successfully developed, how soon the pandemic will end depends on their rollout, as well as other factors. Estimates range from as optimistic as Fall 2021 for the US to as conservative as a few years for the world.[5] For our exercises, we assume that the pandemic ends in two years ($t = 730$) from January 1, 2020. So, π_i^N and π_i^I are set to 0 for $t > 730$, and thus the effective reproduction number also becomes 0. Since COVID-19 is no longer contagious, containment policies are scrapped for $t > 730$. Note that the disease evolution does not immediately end at $t = 730$, as it takes some time for infectious people to move to the next state (recovery or death).

It is infeasible to compute optimal policy by optimizing over the entire time path of containment policies for each of the 42 countries in this full-fledged quantitative model of trade. To tackle this problem, we use the effective reproduction number as the policy target. This is a reasonable target/representation as it reflects the speed of disease spread and is the central concern for epidemiologists and doctors who lead government responses. In addition, targeting an effective reproduction number implies that the containment measures should be stringent initially and gradually relaxed over time, which is a pattern found in several recent studies in the macroeconomic literature which focus on the dynamics of optimal policies in closed-economy contexts; see, e.g., Alvarez et al. (2020) and Jones et al. (2020). This is because the fraction of

[5]Powell A. "Fauci says herd immunity possible by fall, 'normality' by end of 2021" The Havard Gazzet, December 10, 2020 https://news.harvard.edu/gazette/ and The Lancet Microbe (2021)

Susceptible in the population $S_{i,t}/N_i$ diminishes over time; with a fixed target for $R_{e,i,t}$, this implies that containment measures $\eta_{i,t}$ generally decrease over time, provided that the over-time variability of $R_{0,i,t}$ is modest.

To compare with optimal policies, we compute a long-run baseline case in which countries are assumed to keep doing what they have been doing. That is, their policies from November 17, 2020 onward are projected to entail their realized averages of $R_{e,i,t}$ for the period from the onset of the outbreak t_i^* to November 16. Their actual policies up to November 16 are used in simulating the baseline.

We examine optimal policies in two steps. In the first step, we consider a simpler problem in which a global social planner decides an effective reproduction number $\widetilde{R}_e$ that applies to all countries such that the global welfare is maximized. In the second step, we explore individual country's optimal policies. The two steps are useful in two senses: first, the global problem yields a message that would otherwise be obscured in cross-country comparisons; second, the first step helps ease the computational burden for the second step.

Suppose a global social planner decides on an effective reproduction number $\widetilde{R}_e$ such that all countries set up their containment policies $\widetilde{\eta}_{i,t}$ to match $\widetilde{R}_e$, whenever possible. Namely, for each country i, $\{\widetilde{\eta}_{i,t}\}_{t=t_i^*}^{730}$ satisfy

$$R_{e,i,t} = (1-\widetilde{\eta}_{i,t})\left[\pi_i^I + \pi_i^L \sum_{j=1}^{J}(1-\mu_i^j)\ell_{i,t}^j\right] \times 18 \times \frac{S_{i,t}}{N_i} \leq \widetilde{R}_e, \tag{13}$$

where the equality holds if a positive solution of $\widetilde{\eta}_{i,t}$ exists; otherwise $\widetilde{\eta}_{i,t} = 0$ and the inequality holds. Also, $\widetilde{\eta}_{i,t} = \eta_{i,t}$ for $t < t_i^*$,[6] and $\widetilde{\eta}_{i,t} = 0$ for $t > 730$. The goal of the social planner is to maximize long-run global welfare specified in (11).

4.2 Optimal Uniform Effective Reproduction Number for Global Welfare

Using grid search, the uniform effective reproduction number that maximizes global welfare is $\widetilde{R}^*_{e,\text{welfare}} = 0.893$; that which maximizes global real income is $\widetilde{R}^*_{e,\text{income}} = 0.918$. Both are smaller than 1. Figure 2 shows the global welfare and real income in $\widetilde{R}_e$. Several observations are in order. First, on both sides of the optimal points, the slopes are rather steep. Second, there is a drastic difference between welfare and real income when $\widetilde{R}_e$ is near a complete laissez-faire policy (when $\widetilde{R}_e$ is greater than 4.7, most countries' $\widetilde{\eta}_{i,t}$ are 0, and the remaining few are near 0). The global real income is actually higher than the baseline by nearly 1%, even though it is still lower than what would result under the optimal uniform rate. As to the global welfare, the

[6] Note that it is possible that for those days between January 1, 2020 and the onset of the disease evolution, a country may already adopt some containment measures such as border control.

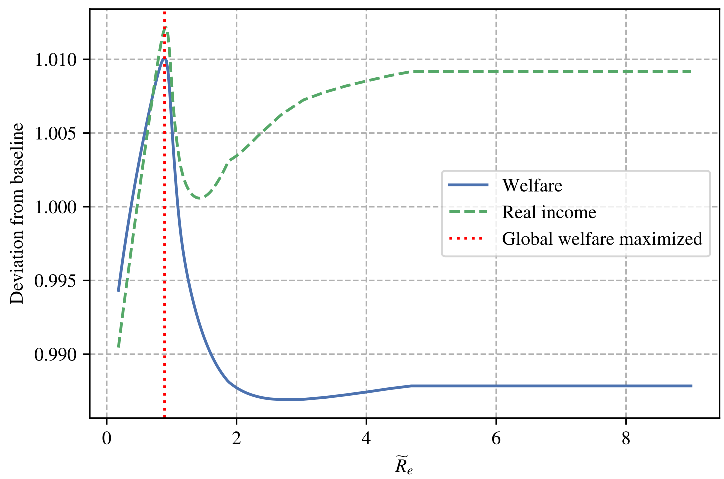

Figure 2: Deviation from the baseline: Global welfare and real income under $\widetilde{R}_e$

laissez-faire policy fares worse (more than 1% lower than the baseline). This gap is not trivial considering this is an impact on long-run welfare from the shocks in a two-year plus period.[7] The main reason for this gap is that deaths are extreme outcomes disliked by risk averse agents; even though there are real-income gains under laissez-faire policies compared with the baseline case, the cost of mortality is amplified in welfare terms so that it overcomes the real-income gains to entail a welfare loss.

One naturally wonders whether individual countries' welfare actually improves under $\widetilde{R}^*_{e,\text{welfare}}$. Figure 4 shows the welfare and real-income improvements by country under $\widetilde{R}^*_{e,\text{welfare}}$. Compared with the baseline, all countries' real income improves, and the welfare of all but five countries improves. Those exceptions are all minor deteriorations, whereas the improvements for many countries are substantial.

4.3 National Social Planners and Optimal Effective Reproduction Numbers

We now consider optimal policies such that each national planner maximizes the country's welfare by choosing the country's effective reproduction number $\widetilde{R}_{e,i}$ (containment policy is solved accordingly in a similar fashion to [13]) given other national planners' choices. The solution is, indeed, a Nash equilibrium of optimal national policies.

Given that $\widetilde{R}^*_e$ set by the global planner already improves most countries' welfare and real income, the information from that exercise is useful for our algorithm of finding a Nash equilibrium of optimal national policies. In particular, it turns out the plot of each individual country's welfare exhibits similar shapes to that in Figure 2. Moreover, the effective reproduction number

[7] We let the simulation run about 200 more days after an effective vaccine is available so that epidemiological evolution gradually subsides such that $I_{i,t} \to 0$ for all countries.

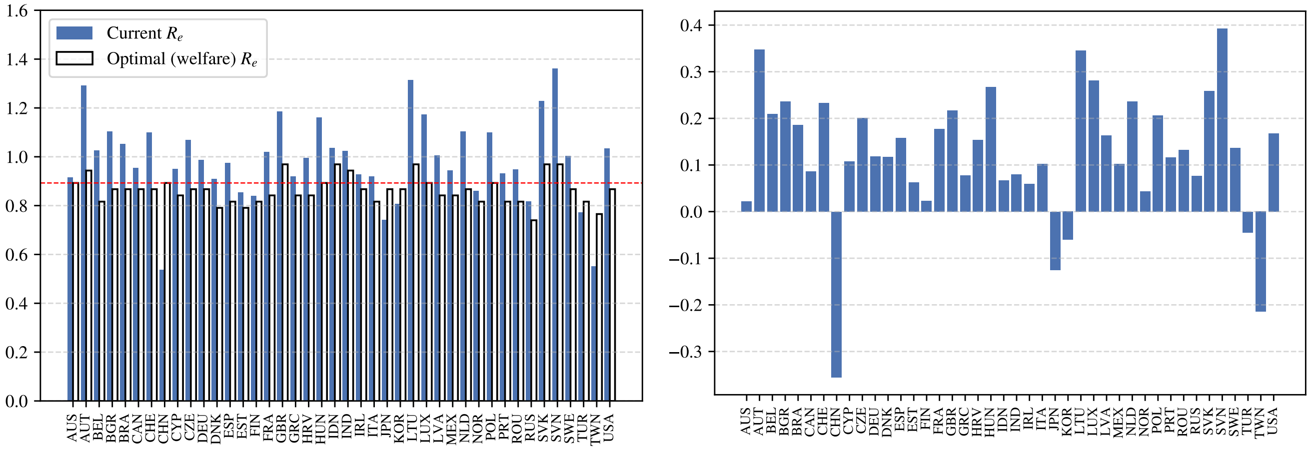

(a) Current $\bar{R}_{e,i}$ and optimal $\widetilde{R}^*_{e,i}$

(b) Deviation of $\bar{R}_{e,i}$ from $\widetilde{R}^*_{e,i}$

Figure 3: Optimal Effective Reproduction Numbers vs Actual Ones

under which the highest welfare for each country is attained is rather close to $\widetilde{R}^*_{e,\text{welfare}}$; such a number is what each national planner would choose if she could set the uniform $\widetilde{R}_e$. Thus, these numbers are chosen as the initial guess for the iterations for finding a Nash equilibrium, a fixed point of best responses (optimal national policies). Along with other information from the previous subsection, this suggests that the optimal $\widetilde{R}^*_{e,i}$ for each national planner is likely found in the neighborhood of the initial guess. Thus, in our grid search, the grids are much denser in that neighborhood and sparser far away from it. This substantially eases the computational burden. Still, the grid search covers the entire range from a total lock-down to a laissez-faire policy.

Figure 3 shows the optimal $\widetilde{R}^*_{e,i}$ compared with the current effective reproduction numbers $\bar{R}_{e,i}$, defined as the over-time average of realized $\{R_{e,i,t}\}$; the uniform optimal number $\widetilde{R}^*_e$ is shown by the red dashed line in Panel (a). Panel (b) shows the difference directly. Several observations are in order. First, all of the $\widetilde{R}^*_{e,i}$'s are less than 1, except those for India and Lithuania. Second, the optimal number $\widetilde{R}^*_{e,i}$ is relatively close to the optimal uniform number $\widetilde{R}^*_e$, as it can be seen clearly that the variation in optimal $\widetilde{R}^*_{e,i}$ is much smaller than that in actual $\bar{R}_{e,i}$. Third, a majority of countries need to tighten up, whereas five countries need to relax. There is a high degree of overlap between the set of countries that need to tighten up significantly and those whose disease spreads are much faster (high effective reproduction number $\bar{R}_{e,i}$; see Figure 1[b]). Fourth, as we intentionally leave out the psychological cost of mortality, once this cost is incorporated, then those that should tighten up should definitely tighten up even more, whereas the conclusion for those that need to relax may become ambiguous.

Unlike in the case under optimal uniform $\widetilde{R}^*_e$, all countries' welfare and real income improve under optimal national policies as shown in Figure 4. For the above-mentioned 20 countries that need to tighten up significantly, their welfare gains are all substantial, more than 1.9% except

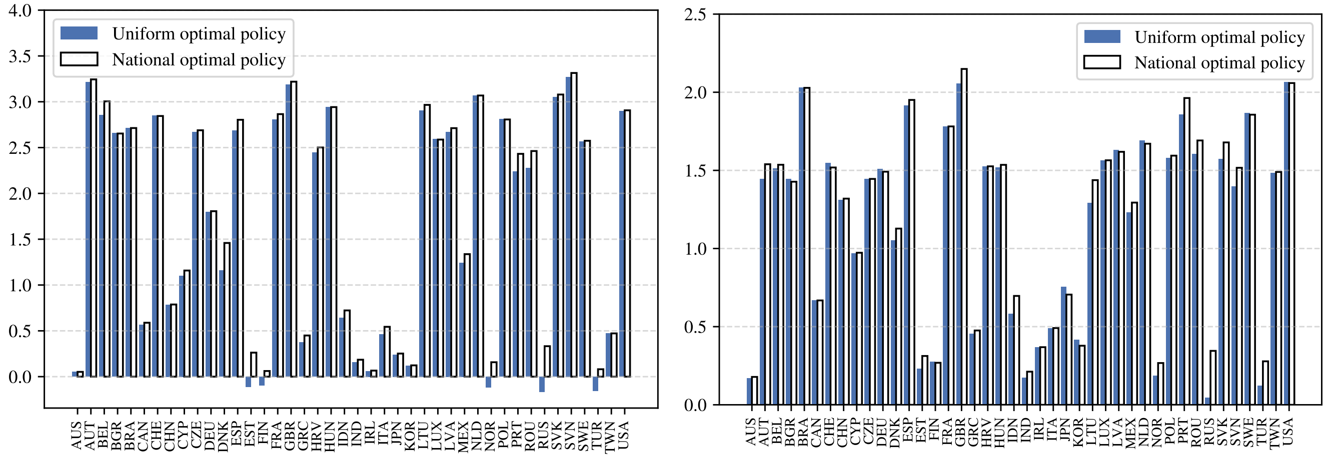

(a) Welfare improvements from the baseline

(b) Real-income improvements from the baseline

Figure 4: Welfare and Real-Income Improvements Under Optimal Policies

Lithuania and more than 2.5% except Bulgaria, Germany, and Lithuania. It is worth emphasizing that these greater than 2.5% long-run welfare gains come merely from policy adjustments of a relatively short period (two years plus).

There is an interesting asymmetry in welfare gains between those countries that need to tighten up and those that need to relax, as the gains in the former are much larger. To comprehend this, it is critical to understand that the long-run cost of mortality factors in both the real income and welfare, but weighs more in welfare because a larger probability of death worsens the expected utility as risk averse agents dislike extreme outcomes. Those countries that need to tighten up are those that also have suffered from faster disease spreads, which indicate high costs of mortality and explain why the welfare gains in these countries are larger than the real-income gains. On the other hand, for countries that need to relax, some can also gain substantially in real income (China and Taiwan, and South Korea to a smaller extent). However, as relaxation implies more deaths, the welfare gains are thus dampened.

4.4 The Role of International Trade

We conduct two counter-factual exercises to examine the role of international trade in our quantitative analysis. First, we examine whether trade mitigates or amplifies the losses from COVID shocks and how this is related to WFH capacities. Second, we examine the changes in optimal policies when countries are shut-down to autarky.

In the first exercise, we first compute equilibrium long-run welfare when all COVID shocks are absent (no disease evolution or containment measures) under trade and under autarky. In Figure 5, the vertical axis is the ratio of the percentage welfare loss from COVID shocks under

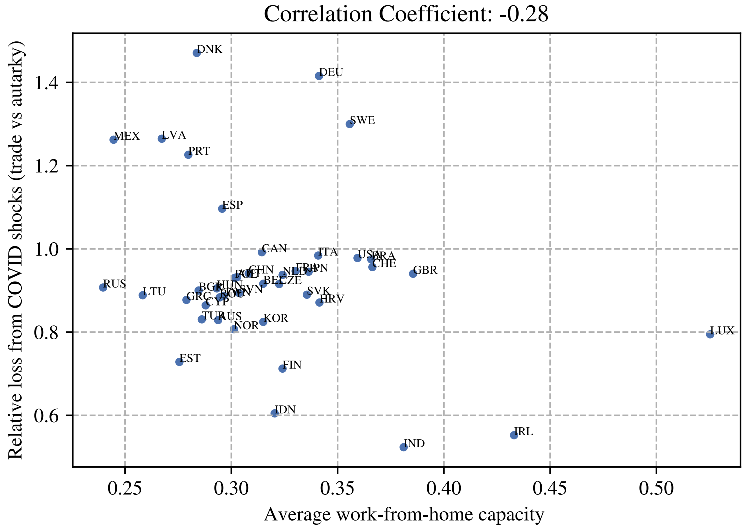

Figure 5: WFH capacity and relative loss from COVID shocks (trade vs autarky)

trade to that under autarky, and the horizontal axis is the country-level average WFH capacity, weighted by pre-COVID sectoral employment shares; that is, $\bar{\mu}_{i,0} = \sum_j \mu_i^j \ell_{i,0}^j$. Despite the model's complexity, we find a negative correlation between the degree of a country's WFH capacity and whether trade helps mitigate COVID shocks. To see this, recall the pandemic shock parameter $B_{i,t}^j = 1 - \eta_{i,t}(1 - \mu_i^j) \in [0, 1]$ and its role in determining trade shares in (8). When there is no pandemic ($\eta_{i,t} = 0$), WFH capacities play no role. During the pandemic, a country with a high initial average WFH capacity gains comparative advantages in high-WFH sectors, and the employment shares in these sectors expand. Thus, trade generally acts as a buffer for these countries. Interestingly, trade can amplify losses from COVID shocks for a small set of countries (7 out of 42) with relatively low average WFH capacities. International specialization induces these countries to specialize in low-WFH sectors, and when combined with stringent containment measures, the losses can be larger than those in autarky.

In the second exercise, we examine how much optimal national policies would change when countries become autarkies. This exercise actually computes the optimal policies as if each country were its own closed economy. Figure 6(a) shows the deviation in optimal $\widetilde{R}_{e,i}^*$ under trade from that under autarky. Due to complex trade linkages, there is no unanimous sign of the deviation. However, more countries' (34 out of 42) optimal $\widetilde{R}_{e,i}^*$ under trade are lower than that under autarky; for those countries whose optimal $\widetilde{R}_{e,i}^*$ under trade should be higher, the deviations are rather small except those of India and Indonesia. These indicate that optimal containment policies are generally tighter under trade than under autarky. This is because gains from trade generally imply more room to buffer pandemic shocks from sourcing intermediate inputs or purchasing final goods from foreign countries, resulting in larger real income and welfare under

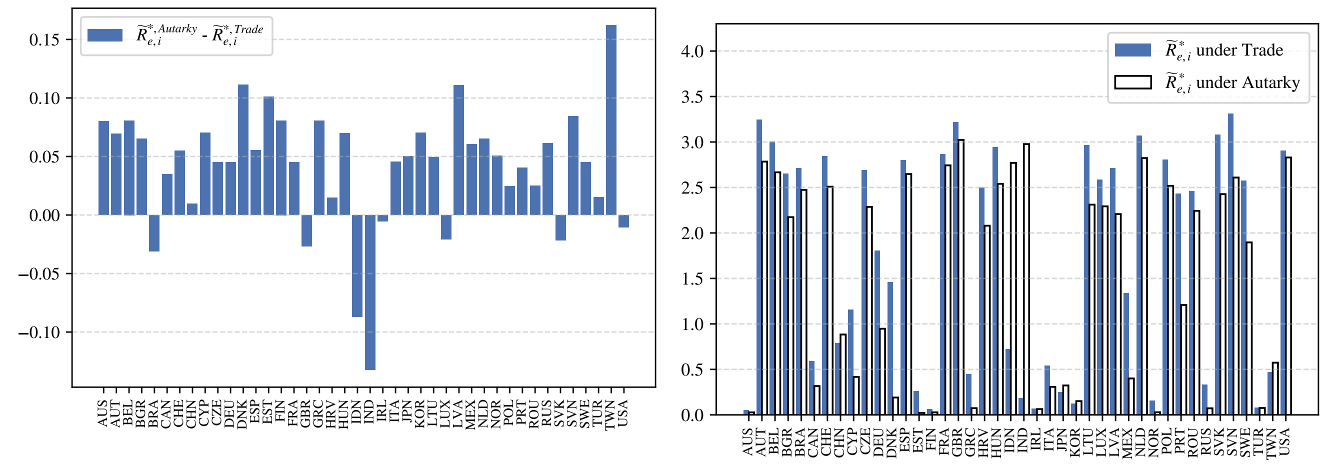

(a) Deviation in optimal $\widetilde{R}^{*}_{e,i}$ under trade from that under autarky

(b) Welfare improvement (trade vs autarky)

Figure 6: Comparison of Optimal Policies between Trade and Autarky

trade. On the tradeoff between lives and economies, national planners can thus afford to adopt more stringent policies for long-run gains by saving lives as short-run losses in production and income are less under trade.

Figure 6(b) shows the welfare improvements under optimal policies compared with the baseline in both open-economy and closed-economy scenarios. For some countries, the differences in welfare improvements between the two scenarios are rather large. To further examine the magnitudes of the differences, we calculate the relative difference in absolute value for each country by

$$\frac{|\text{Welfare Improvement under Autarky - Welfare Improvement under Trade}|}{\text{Welfare Improvement under Trade}}.$$

The average relative difference is 0.72, i.e., the average difference is 72% relative to the welfare improvement under trade. The corresponding standard deviation is 2.30, indicating large variation across countries. Thus, incorporating trade is important and quantitatively relevant.

5 Conclusion

The novelty of this work is to use the effective reproduction numbers as policy targets to reduce the space of candidate policies in a model with rich cross-sectional links across countries and sectors and with these links interacting with disease dynamics. Our quantitative analyses prove to be informative; the takeaway messages are as follows.

First, as highlighted by the global planner's problem, a laissez-faire policy might not be all that bad in terms of long-run real income, but it is a drastically worse policy in welfare terms because of risk aversion. Second, in terms of optimal national policies, a majority of countries need to tighten up, whereas only a handful of countries need to relax. An interesting asymmetry is that substantial welfare gains occur only in the countries that need to tighten up significantly. Psychological costs of mortality are intentionally left out of the model. When such costs are incorporated, those countries that should tighten up should tighten up even more, and the welfare implications are even larger. Third, international trade acts as a buffer to welfare losses from the pandemic if a country's average WFH capacity is high, and it also implies substantially different optimal policies in welfare terms from closed-economy settings.

References

Acemoglu, D., Chernozhukov, V., Werning, I., and Whinston, M. D. (2020). Optimal Targeted Lockdowns in a Multi-Group SIR Model. NBER Working Paper 27102.

Alvarez, F. E., Argente, D., and Lippi, F. (2020). A Simple Planning Problem for COVID-19 Lockdown. NBER Working Paper 26981. forthcoming at *American Economic Review: Insights*.

Antrás, P., Redding, S. J., and Rossi-Hansberg, E. (2020). Globalization and Pandemics. NBER Working Paper 27840.

Argente, D. O., Hsieh, C.-T., and Lee, M. (2020). The Cost of Privacy: Welfare Effects of the Disclosure of COVID-19 Cases. NBER Working Paper 27220.

Atkeson, A. (2020). On using SIR Models to Model Disease Scenarios for COVID-19. *Quarterly Review*, 41(1):1–35. Federal Reserve Bank of Minneapolis.

Atkeson, A. G., Kopecky, K., and Zha, T. (2020). Behavior and the Transmission of COVID-19. AEA Papers and Proceedings. forthcoming.

Bonadio, B., Huo, Z., Levchenko, A. A., and Pandalai-Nayar, N. (2020). Global Supply Chains in the Pandemic. NBER Working Paper 27224.

Budish, E. B. (2020). Maximize utility subject to $R \leq 1$: A Simple Price-theory Approach to COVID-19 Lockdown and Reopening Policy. NBER Working Paper 28093.

Caliendo, L. and Parro, F. (2015). Estimates of the Trade and Welfare Effects of NAFTA. *The Review of Economic Studies*, 82(1):1–44.

Chen, J., Chen, W., Liu, E., Luo, J., and Song, Z. M. (2020). The Economic Impact of COVID-19 in China: Evidence from City-to-City Truck Flows. Working Paper, Princeton University.

Dingel, J. I. and Neiman, B. (2020). How Many Jobs Can be Done at Home? *Journal of Public Economics*, 189:104235.

Dong, E., Du, H., and Gardner, L. (2020). An interactive web-based dashboard to track covid-19 in real time. *The Lancet infectious diseases*, 20(5):533–534.

Eaton, J. and Kortum, S. (2002). Technology, Geography, and Trade. *Econometrica*, pages 1741–1779.

Eichenbaum, M. S., Rebelo, S., and Trabandt, M. (2020). The Macroeconomics of Epidemics. NBER Working Paper 26882. forthcoming at *Review of Financial Studies*.

Eppinger, P., Felbermayr, G., Krebs, O., and Kukharskyy, B. (2020). COVID-19 Shocking Global Value Chains. Cesifo working paper.

Fajgelbaum, P., Khandelwal, A., Kim, W., Mantovani, C., and Schaal, E. (2020). Optimal Lockdown in a Commuting Network. NBER Working Paper 27441.

Farboodi, M., Jarosch, G., and Shimer, R. (2020). Internal and External Effects of Social Distancing in a Pandemic. NBER Working Paper 27059.

Hale, T., Angrist, N., Cameron-Blake, E., Hallas, L., Kira, B., Majumdar, S., Petherick, A., Phillips, T., Tatlow, H., and Webster, S. (2020). Oxford COVID-19 Government Response Tracker. *Blavatnik School of Government*.

Head, K. and Mayer, T. (2014). Gravity equations: Workhorse, toolkit, and cookbook. In *Handbook of International Economics*, volume 4, pages 131–195. Elsevier.

Jones, C. J., Philippon, T., and Venkateswaran, V. (2020). Optimal Mitigation Policies in a Pandemic: Social Distancing and Working from Home. NBER Working Papers 26984.

Kermack, W. O., McKendrick, A. G., and Walker, G. T. (1927). A Contribution to the Mathematical Theory of Epidemics. *Proceedings of the Royal Society of London. Series A, Containing Papers of a Mathematical and Physical Character*, 115(772):700–721.

Krueger, D., Uhlig, H., and Xie, T. (2020). Macroeconomic Dynamics and Reallocation in an Epidemic. NBER Working Paper 27047.

Liang, L.-L., Tseng, C.-H., Ho, H. J., and Wu, C.-Y. (2020). Covid-19 Mortality is Negatively Associated with Test Number and Government Effectiveness. *Scientific Reports*, 10(12567).

Low, H. and Pistaferri, L. (2015). Disability Insurance and the Dynamics of the Incentive Insurance Trade-Off. *American Economic Review*, 105(10):2986–3029.

Mayer, T. and Zignago, S. (2011). Notes on CEPII's Distances Measures: The GeoDist database.

Piguillem, F. and Shi, L. (2020). Optimal COVID-19 Quarantine and Testing Policies. EIEF Working Papers Series 2004, Einaudi Institute for Economics and Finance (EIEF).

Simonovska, I. and Waugh, M. E. (2014). The Elasticity of Trade: Estimates and Evidence. *Journal of International Economics*, 92(1):34 – 50.

The Lancet Microbe (2021). Covid-19 vaccines: the pandemic will not end overnight. *The Lancet Microbe*, 2(1):e1.

Timmer, M. P., Dietzenbacher, E., Los, B., Stehrer, R., and De Vries, G. J. (2015). An illustrated user guide to the world input–output database: the case of global automotive production. *Review of International Economics*, 23(3):575–605.

WHO (2020). Coronavirus disease 2019 (covid-19): situation report, 46.

Appendix

A Quantification

Our model consists of two sets of parameters: economic and epidemiological. We describe how they are calibrated in order.

A.1 Economic Parameters

A.1.1 Risk aversion and time preference

For our quantitative analyses, we set the per-period utility as

$$u(q) = \frac{(q+1)^{1-\sigma} - 1}{1-\sigma}.$$

We choose this functional form for three reasons. First, this specification is similar to the CRRA (constant relative risk aversion) utility if the term $q+1$ is replaced with q. Thus, it is approximately CRRA when q is large; the parameter σ measures the degree of relative risk aversion. Second, $u(0) = 0$, which satisfies our requirement that psychological costs be left out of the model; note that the exact CRRA utility entails $\lim_{q \to 0} u(q) \to -\infty$ when $\sigma \geq 1$ and is therefore not implementable. Third, $\sigma = 0$ corresponds to the risk-neutral case. Following Low and Pistaferri (2015), the relative risk aversion σ is set to 1.5. Following Farboodi et al. (2020), we set the annual discount rate as 0.95; as daily data is used, $\rho = 0.95^{\frac{1}{365}} \approx 0.99986$.

A.1.2 WIOD

Our main data source is the World Input-Output Database (WIOD), which contains information on bilateral trade for intermediates and for final goods for 43 countries and 56 industries. The country of Malta is dropped as it is not included in the data on containment policy from the Oxford COVID-19 Government Response Tracker. Table 1 lists the 42 countries in the data. We use the data from the year 2014, the latest available year from WIOD, and aggregate 56 industries into 6 sectors. See Table 2 for the list of industries and sectors. Two industries are left out of our aggregation (activities of households as employers and activities of extraterritorial organizations and bodies) since there is no corresponding work-from-home capability in Dingel and Neiman (2020).

Under the Social Economic Account, the database also provides information on total labor compensation and the total number of persons engaged for each industry; these allow for calculating country-specific wages. See Timmer et al. (2015).

Also, from WIOD, we obtain data on gross production across countries and sectors, as well as each sector-j's use of intermediates across countries and sectors. The data also include sectoral final consumption across countries. We can therefore compute the shares of intermediate use $\gamma_i^{j,l}$ as the shares of total intermediate use by sector j on goods from sector l. The final consumption shares α_i^j are computed by total sector-j final consumption over the total final consumption. The shares of intermediate in gross output, $1-\beta_i^j$, are calculated by the total intermediate use over the gross production.

A.1.3 Estimation of productivity parameters $\{T_i^j\}$ and trade costs $\{\tau_{i,n}^j\}$

Given the data on trade shares and geography from the WIOD and Centre d'Études Prospectives et d'Informations Internationales (CEPII), the model's gravity equations and hence trade costs $\{\tau_{i,n}^j\}$ can be estimated. Following Simonovska and Waugh (2014), we set the value of trade elasticity $\theta = 4$. Given trade elasticity, estimated trade costs, various share parameters $\{\alpha_i^j, \beta_i^j, \gamma_i^{j,l}\}$, and data on wages obtained from the Social Economic Account in WIOD, the productivity parameters $\{T_i^j\}$ can then be backed out using the model structure. We describe the estimation of trade costs and productivity parameters in order.

Gravity Equation We use a standard approach in estimating productivity parameters $\{T_i^j\}$ and trade costs $\tau_{i,n}^j$. Start with the model's gravity equation:

$$X_{i,n}^j = \frac{T_i^j (c_i^j \tau_i^j)^{-\theta}}{\Phi_n^j} X_n^j.$$

Taking the logarithm of both sides, we have

$$\ln X_{i,n}^j = \ln[T_i^j (c_i^j)^{-\theta}] + \ln[(\tau_{i,n}^j)^{-\theta}] + \ln[X_n^j (\Phi_n^j)^{-1}].$$

Assume that trade costs take the functional form below,

$$-\theta \ln \tau_{i,n}^j = \nu_0^j \ln(dist_{i,n}) + \nu_2^j contig_{i,n} + \nu_3^j comlang_{i,n} + \nu_4^j colony_{i,n},$$

where $dist_{i,n}$ is the distance between i and n in thousands of kilometers, and $contig_{i,n}$ equals one if countries i and n share a border. Analogously, $comlang_{i,n}$ and $colony_{i,n}$ indicate whether two countries share the same language and colonial historical links. These variables are obtained from the GeoDist database from the Centre d'Etudes Prospectives et d'Informations Internationales (CEPII) (see Mayer and Zignago (2011)). Thus, the empirical specification is

$$\ln X_{i,n}^j = \nu_0^j \ln(dist_{i,n}) + \nu_2^j contig_{i,n} + \nu_3^j comlang_{i,n} + \nu_4^j colony_{i,n} + D_i^{j,exp} + D_n^{j,imp} + \varepsilon_{i,n}^j$$

Following Head and Mayer (2014), we apply OLS to estimate the fixed effects model to obtain estimates of $\{\nu^j, D_i^{j,exp}\}$.

Uncovering Productivity Parameters We set $\theta = 4$, following the trade literature, in particular Simonovska and Waugh (2014). Trade costs $\{\tau_{i,n}^j\}$ can be calculated using the estimated coefficients:

$$\hat{\tau}_{i,n}^j = \exp\left(\frac{\hat{\nu}_0^j \ln(dist_{i,n}) + \hat{\nu}_2^j contig_{i,n} + \hat{\nu}_3^j comlang_{i,n} + \hat{\nu}_4^j colony_{i,n}}{-\theta}\right).$$

Then, we use the estimated exporter dummies and data on wages to obtain T_i^j by the following procedure. First, observe that

$$\hat{T}_i^j = \exp(\hat{D}_i^{j,exp}) \times (c_i^j)^\theta,$$

where $c_i^j = w_i^{\beta_i^j}(P_i^{M,j})^{1-\beta_i^j}$ is the unit cost of production. As mentioned in Appendix A.1.2, wages w_i are observed from the Social Economic Account in the WIOD. Hence,

$$\hat{T}_i^j = \exp(\hat{D}_i^{j,exp}) \times [w_{i,data}^{\beta_i^j}(\hat{P}_i^{M,j})^{1-\beta_i^j}]^\theta \tag{14}$$

$$\hat{P}_i^{M,j} = \prod_{l=1}^{J}(\hat{P}_i^l)^{\gamma_i^{j,l}} \tag{15}$$

$$\hat{P}_i^j = \Gamma\left(\frac{\theta - 1 + \kappa}{\theta}\right)\left[\sum_{k=1}^{K} \hat{T}_k^j [w_{i,data}^{\beta_i^j}(\hat{P}_i^{M,j})^{1-\beta_i^j}\hat{\tau}_{i,k}^j]^{-\theta}\right]^{-\frac{1}{\theta}}. \tag{16}$$

The following procedure is used to solve for $\{T_i^j\}$. Let r index the rounds of iterations, and start with an initial guess of $\{\hat{P}_i^{M,j}(0)\}$.

1. Update productivity: $\hat{T}_i^j(r) = \exp(\hat{D}_i^{j,exp}) \times [w_{i,data}^{\beta_i^j}\hat{P}_i^{M,j}(r)^{1-\beta_i^j}]^\theta$.

2. Update sectoral price indices: $\hat{P}_i^j(r) = \Gamma\left(\frac{\theta - 1 + \kappa}{\theta}\right)\left[\sum_{k=1}^K \hat{T}_k^j(r)(w_{i,data}^{\beta_i^j}\hat{P}_i^{M,j}(r)^{1-\beta_i^j}\hat{\tau}_{i,k}^j)^{-\theta}\right]^{-\frac{1}{\theta}}$.

3. Update the price indices of the intermediate-input bundle: $\hat{P}_i^{M,j}(r+1) = \prod_{l=1}^J[\hat{P}_i^l(r)]^{\gamma_i^{j,l}}$.

4. Stop the iterations if

   $$||\hat{P}_i^{M,j}(r+1) - \hat{P}_i^{M,j}(r)|| < tolerance.$$

   Otherwise, go back to Step 1.

5. Take $\hat{T}_i^j = \hat{T}_i^j(r+1)$ as our estimates of country-sector-specific productivity parameters.

For the model without input-output linkages, the calibration is the same except that $\beta_i^j = 1$ in (14) and (16), and that (15) is not used.

A.1.4 Work-from-home capacity

To measure work-from-home capacity by industry, we use the data from Dingel and Neiman (2020), who compute work-from-home capacity by occupation. We use the data aggregated to the 3-digit NAICS and adopt the version in which each occupation's capacity was manually assigned by these authors by inspecting the definitions of the occupations. Our results remain similar when using the other version, which is algorithm-based. The data was downloaded from `https://github.com/jdingel/DingelNeiman-workathome`.

To calculate each WIOD industry's work-from-home capacity, we map each WIOD industry to one or multiple 3-digit NAICS industries according to their definitions. Six WIOD industries map directly into two-digit NAICS, in which cases the 2-digit NAICS work-from-home capacity computed by these authors are used. When a WIOD industry maps into multiple NAICS industries, we proxy the WIOD industry's work-from-home capacity by the average across the corresponding NAICS industries weighted by their industrial employment. The industrial employment data is obtained from the Quarterly Workforce Indicators (QWI) under the LEHD program of the Census Bureau (`https://ledextract.ces.census.gov/static/data.html`); the fourth quarter of 2014 was used as our WIOD data is for 2014. By-industry and by-state employment data is obtained from QWI, and the industrial employment is the sum across all states. This procedure creates a $\{\mu^j\}$ for WIOD industries.

In our aggregation of WIOD industries into six sectors, the work-from-home capacity for each country-sector pair μ_i^j is computed as the average of these capacities across industries in that sector, weighted by the industrial employment in that country given from the WIOD data.

A.1.5 Containment measures

The containment measures $\{\eta_{i,t}\}$ across countries and time are directly obtained from the *Stringency Index* by the Oxford COVID-19 Government Response Tracker (OxCGRT; Hale et al. 2020) at a daily frequency. This index summarizes a government's responses in terms of various closures and containment, including school or workplace closures, stay-at-home requirements, border control, and restrictions on gathering, public events, public transport, and internal movements, as well as public information campaigns.[8]

[8]For more details, see Hale et al. (2020) and `https://www.bsg.ox.ac.uk/research/research-projects/coronavirus-government-response-tracker`.

A.2 Epidemiological Parameters

The epidemiological parameters to be calibrated are $\{\pi^r, \pi^d, \delta, \pi_i^I, \pi_i^L, \alpha^I, I_{i,0}\}$. As in Atkeson (2020) and several other macro-SIR models, we set

$$\pi^r + \pi^d = \frac{1}{18} \ \forall i, \tag{17}$$

which means that it takes on average 18 days to either recover or die from the infection.

From Liang et al. (2020), the base mortality rate is set at $\pi^d = 0.037 \times \frac{1}{18}$.[9] Following Alvarez et al. (2020), we set $\delta = 0.05 \times \frac{1}{18}$. As a WHO (2020) COVID-19 Situation Report indicates that asymptotic and mild cases account for about 80% of the infections, we set $\alpha^I = 0.8$.

For our purpose, it is important to quantify infection probabilities $\{\pi_i^I, \pi_i^L\}$, as they are the key parameters underlying the variations in the rate of disease reproduction across countries, besides economic conditions and containment policies. Also, for the epidemiological evolution to commence, an estimate of $I_{i,0}$ is required (as $S_{i,0} = N_i - I_{i,0}$ and $R_{i,0} = D_{i,0} = 0$); $I_{i,0}$ is generally unknown because the society might be unaware of, unprepared for, or on low alert for the disease, so that the number of the first few reported cases may be quite off. To estimate the country-specific infection parameters $\{\pi_i^I, \pi_i^L, I_{i,0}\}$, we will use non-linear least squares to fit the data of total confirmed cases for each country. Note that, however, calculating total confirmed cases in this global economy where countries are interlinked in various ways as explained in the main text is time-consuming; hence such estimation is infeasible. In particular, the sectoral employment shares $\{\ell_{i,t}^j\}$ are time-varying and determined by the entire vector $\{\pi_i^I, \pi_i^L, I_{i,0}\}_{i=1}^{42}$ for all 42 countries. Thus, the space of candidate estimates is too large to be feasible.

Thus, we adopt a simpler approach to estimate $\{\pi_i^I, \pi_i^L, I_{i,0}\}$ by proxying sectoral employment shares $\{\ell_{i,t}^j\}$ by such shares in the pre-COVID-19 global economy $\{\ell_i^{j,\text{pre}}\}$. Then, the effective reproduction number becomes

$$\begin{aligned} R_{e,i,t} \equiv \frac{T_{i,t}}{I_{i,t}} \times 18 &= (1 - \eta_{i,t}) \left[\pi_i^I + \pi_i^L \times \sum_{j=1}^{J} (1 - \mu_i^j) \ell_i^{j,\text{pre}} \right] \times 18 \times \frac{S_{i,t}}{N_i} \\ &\equiv (1 - \eta_{i,t}) \times R_{0,i} \times \frac{S_{i,t}}{N_i}. \end{aligned}$$

When the disease dynamics are modified this way, the estimation can be done country by country, and the basic reproduction number $R_{0,i,t}$ also becomes a constant $R_{0,i}$. We first estimate the rates of transmission and initial infections, $\{R_{0,i}, I_{i,0}\}$, simultaneously, and then back out infection probabilities $\{\pi_i^I, \pi_i^L\}$.

[9] This number is estimated as a case mortality rate. This choice of mortality rate is consistent with our estimation of key parameters using official data on the number of cases as described below.

Let t_i^* denote the first date on which country i's number of total confirmed cases exceeds 50, and assume that the previous day $t_i^* - 1$ is when $I_{i,0}$ is applied. Let T be the latest available data date of the Stringency Index for all countries in our sample (November 16, 2020). For each country i, we estimate the following equation using nonlinear least-squares:

$$(\hat{R}_{0,i}, \hat{I}_{i,0}) = \text{argmin} \sum_{t=t_i^*}^{T} \left[C_{i,t,data} - C_{i,t}(R_{0,i}, I_{i,0}; \boldsymbol{\eta}_{i,T})\right]^2,$$

where $\boldsymbol{\eta}_{i,T}$ is the full history of $\eta_{i,t}$ up to date T, $C_{i,t}$ is the number of total confirmed cases at date t from the model, and $C_{i,t,data}$ is the number of total confirmed cases downloaded from the Humanitarian Data Exchange website.[10] This website compiles data from the Johns Hopkins University Center for Systems Science and Engineering (JHU CCSE), which documents for COVID-19 the numbers of total cases, total deaths, and daily confirmed cases for more than 200 countries and regions.

Borrowing from the results in Eichenbaum et al. (2020), we assume that $2/3$ of the infections come from general activities. With estimated $\{\hat{R}_{0,i}\}$, $\{\pi_i^I, \pi_i^L\}$ can then be solved from

$$\pi_i^I + \pi_i^L \sum_{j=1}^{J} (1-\mu_i^j)\ell_i^{j,\text{pre}} = \frac{\hat{R}_{0,i}}{18}, \tag{18}$$

$$\frac{\pi_i^I}{\pi_i^I + \pi_i^L \sum_{j=1}^{J}(1-\mu_i^j)\ell_i^{j,\text{pre}}} = \frac{2}{3}. \tag{19}$$

Our estimated model fits the data reasonably well, as the cross-country average and standard deviation of R^2 are 0.88 and 0.067, respectively.

Such estimated $\{\hat{R}_{0,i}\}$ are reported in Figure 7. The estimated $R_{0,i}$ ranges from 0.93 (Taiwan) to 5.30 (India), and the average is 2.98. For most countries, the $R_{0,i}$ values fall between 2 and 4. An important feature here is that when estimating $R_{0,i}$ using confirmed cases, the effect of containment measures is incorporated. Hence, the estimated $R_{0,i}$ is separate from the effect from containment policies $1 - \eta_i$.

Note that in our quantitative analyses, the disease dynamics and, in particular, the effective reproduction number $R_{e,i,t}$ are still generated from the full model.

[10] Novel Coronavirus (COVID-19) Cases Data https://data.humdata.org/dataset/novel-coronavirus-2019-ncov-cases.

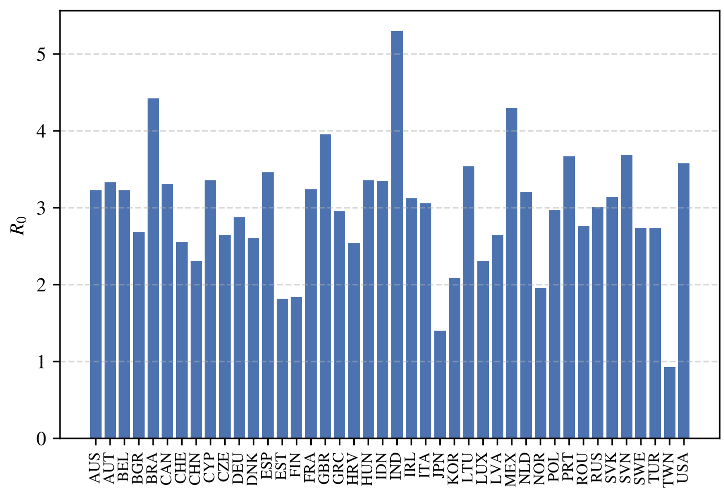

Figure 7: Estimated Basic Reproduction Number $R_{0,i}$

ISO-3 code	Country name	ISO-3 code	Country name
AUS	Australia	IND	India
AUT	Austria	IRL	Ireland
BEL	Belgium	ITA	Italy
BGR	Bulgaria	JPN	Japan
BRA	Brazil	KOR	Republic of Korea
CAN	Canada	LTU	Lithuania
CHE	Switzerland	LUX	Luxembourg
CHN	China	LVA	Latvia
CYP	Cyprus	MEX	Mexico
CZE	Czech Republic	NLD	Netherlands
DEU	Germany	NOR	Norway
DNK	Denmark	POL	Poland
ESP	Spain	PRT	Portugal
EST	Estonia	ROU	Romania
FIN	Finland	RUS	Russian Federation
FRA	France	SVK	Slovakia
GBR	United Kingdom	SVN	Slovenia
GRC	Greece	SWE	Sweden
HRV	Croatia	TUR	Turkey
HUN	Hungary	TWN	Taiwan
IDN	Indonesia	USA	United States

Table 1: List of countries

WIOD description	WIOD code	Industry	WIOD description	WIOD code	Industry
Crop and animal production	A01	Agriculture and mining	Wholesale and retail vehicles	G45	Non-high-skilled service
Forestry and logging	A02	Agriculture and mining	Wholesale trade	G46	Non-high-skilled service
Fishing and aquaculture	A03	Agriculture and mining	Retail trade	G47	Non-high-skilled service
Mining and quarrying	B	Agriculture and mining	Land transport	H49	Non-high-skilled service
Food products, beverages and tobacco products	C10-C12	Food and texile	Water transport	H50	Non-high-skilled service
Textiles, wearing apparel and leather products	C13-C15	Food and texile	Air transport	H51	Non-high-skilled service
Wood and cork	C16	Resource Manufacturing	Warehousing	H52	Non-high-skilled service
Paper products	C17	Resource Manufacturing	Postal activities	H53	Non-high-skilled service
Printing and reproduction of recorded media	C18	Resource Manufacturing	Accommodation and food	I	Non-high-skilled service
Coke and refined petroleum products	C19	Resource Manufacturing	Publishing	J58	High-skilled service
Chemical products	C20	Resource Manufacturing	Media	J59_J60	High-skilled service
Pharmaceutical products	C21	Resource Manufacturing	Telecommunications	J61	High-skilled service
Rubber and plastic products	C22	Resource Manufacturing	Computer and information	J62_J63	High-skilled service
Other non-metallic mineral products	C23	Resource Manufacturing	Financial services	K64	High-skilled service
Basic metals	C24	Manufacturing	Insurance	K65	High-skilled service
Fabricated metal products	C25	Manufacturing	Auxiliary to financial services	K66	High-skilled service
Electronic and optical products	C26	Manufacturing	Real estate	L68	High-skilled service
Electrical equipment	C27	Manufacturing	Legal and accounting	M69_M70	High-skilled service
Machinery and equipment	C28	Manufacturing	Architectural	M71	High-skilled service
Motor vehicles	C29	Manufacturing	Scientific research	M72	High-skilled service
Other transport equipment	C30	Manufacturing	Advertising	M73	High-skilled service
Furniture	C31_C32	Manufacturing	Other professional	M74_M75	High-skilled service
Repair and installation of machinery	C33	Non-high-skilled service	Administrative	N	High-skilled service
Electricity and gas	D35	Non-high-skilled service	Public administration	O84	High-skilled service
Water supply	E36	Non-high-skilled service	Education	P85	High-skilled service
Sewerage and waste	E37-E39	Non-high-skilled service	Human health and social work	Q	High-skilled service
Construction	F	Non-high-skilled service	Other service	R_S	High-skilled service

Table 2: Concordance of WIOD sectors